Recovery of Low Permeability Reservoirs Considering Well Shut-Ins and Surfactant Additivities

Shuai Li [1,2,*](ID) , Jun Tang [3,*](ID) , Yunhong Ding [1] , Shimin Liu [2] , Guangfeng Liu [4] and Bo Cai [1]**

[1] Research Institute of Petroleum Exploration & Development, PetroChina, Beijing 100083, China; dyhong@petrochina.com.cn (Y.D.); caibo69@petrochina.com.cn (B.C.)
[2] Department of Energy and Mineral Engineering, G3 Center and Energy Institute, Pennsylvania State University, University Park, PA 16802, USA; szl245@psu.edu
[3] School of Geosciences, Yangtze University, Wuhan 430100, China
[4] Education Ministry Key Laboratory of Petroleum Engineering, China University of Petroleum, Beijing 102249, China; lgfmail@yeah.net
* Correspondence: ls_cupb@163.com (S.L.); jtang@yangtzeu.edu.cn or tang0262@sina.com (J.T.); Tel.: +1-814-954-9510 (S.L.); Fax: +1-814-865-3248 (S.L.)

Abstract: To investigate the mechanism whereby well shut-ins and surfactant additivities can increase hydrocarbon output after hydraulic fracturing, in this paper, we simulated well shut-ins with one end open (OEO) rock samples and performed a serious of imbibition experiments with different surfactant additivities based on contact angle (CA) and interfacial tension (IFT) measurements. Scanning electron microscope (SEM) and nuclear magnetic resonance (NMR) methods were also been adopted in the detection before and after shut-ins. The results demonstrated that cationic surfactants result in better improving oil recovery (IOR) performance due to their high wettability alteration ability on vertical fracture faces, while different kinds of surfactants have a similar ability in lowering IFT. As for shut-ins duration, the NMR transverse relaxation time (T_2) spectrum move towards the left side, indicating that aqueous phases migrate to smaller pores spaces and deeper distances. Aqueous migration during the shut-ins period can remove near-fracture trapped water, while surfactant additivities can accelerate and enhance this process, and these two points are the most direct reasons for the observed hydrocarbon output increases.

Keywords: low permeability reservoir; hydraulic fracturing; well shut-ins; surfactant additivities; imbibition; wettability alteration

1. Introduction

In recent years, the development of low permeability reservoirs has become a research hotpot because of the key technology breakthroughs of horizontal well drilling and multi-stage hydraulic fracturing [1–3]. To economically extract hydrocarbons from low permeability formations, a large amount of hydraulic fluids must be pumped into the underground reservoirs to create complex fractures and maximize the contact area with the formation [4,5]. It is reported that only 5–50% of these fracturing fluids can be recovered and a large portion would be 'lost' in the underground reservoirs [6,7].

Fracturing fluid loss into formations can cause serious mechanical damage such as clay swelling, solid precipitation and fines migration, which will block the original connected pores and throats and result in physical permeability reduction [8]. What's more, injected fracturing fluids 'trapped' in the near fracture can form a 2-phase seepage resistance and reduce the effective permeability for

the oil phase [9,10]. Fluid loss into formations may result in a fast pressure reduction when depletion has developed in a reservoir, without a pressure supply such as water or gas injection, in which the drawdown pressure must be larger than the capillary pressure to drain pore fluids to the wellbore during the well production process [11]. At the same time, recent studies have shown that hydrocarbon production increased dramatically in Marcellus shale reservoirs when they had undergone 6 months of well shut-ins after hydraulic fracturing [12]. Scholars explain this by aqueous redistribution due to spontaneous imbibition or osmotic pressure [6,7,10–13]. The aqueous phase enters pore spaces and displaces the original oil phase during capillary-dominated counter-current imbibition, decreasing water saturation and increasing the oil phase relative permeability simultaneously [14]. Aqueous phase redistribution and seepage into deeper distances under this imbibition mechanism can be responsible for both fluid losses and low fracturing fluid recovery [15]. However, these explanations are mainly hypothesis or based on previous experience, and no convincing pore scale or visible evidence has been published to demonstrate the underlying mechanism.

Friction reducing agents, stabilizing agents, bactericidal agents and gel breaker agents are traditionally used fracturing fluids additives, while in recent years, drawing on the experience about chemical agents from tertiary oil recovery, several studies have added surfactants into fracturing fluids in case they may have the potential to reduce water losses and increase oil production [16,17]. Scholars usually evaluate chemical fluids' effectiveness in improved oil recovery (IOR) or enhanced oil recovery (EOR) via wettability alteration and IFT reduction [18–20]. When oil-wet rock wettability is altered to water-wet, capillary forces can turn from negative to positive for spontaneous imbibition. Furthermore, IFT reduction can reduce capillary trapped water and it has a potential enhancing effect for near-fracture water removal [21]. Under these conditions, scholars have demonstrated that well shut-ins and surfactant additives are the two effective ways to increase hydrocarbon outputs after hydraulic fracturing [22,23]. Despite the above studies, there still remaining questions regarding well shut-ins and surfactant additives as IOR techniques in low permeability reservoirs. Previous explanations for the mechanism whereby well shut-ins can enhance hydrocarbon production are mainly based on former empirical experience and lack any firm evidence. In addition, even though scholars have evaluated surfactant additives using wettability and IFT parameters, there still no unified quantitative method to describe their efficacy and applicability.

In this paper, we investigated the inner mechanism explaining why well shut-ins and surfactant additives can improve hydrocarbon output after hydraulic fracturing. We combined different kinds of surfactants into slickwater and performed a serious of OEO imbibition experiments to simulate well shut-ins. SEM and NMR methods have been used to investigate the aqueous phase migration before and after well shut-ins. In addition, we propose a new parameter combining wettability and IFT to evaluate surfactant additive effectiveness.

2. Methodology

When underground reservoir rocks are saturated in an oil environment, organic acid reactions, colloidal and asphaltene adsorption will make the rocks present oil-wet characteristics, while when these oil-wet rocks are then placed into surfactant fluids, their wettability may change [24]. To evaluate the efficiency of different surfactants in oil recovery after shut-ins, we performed OEO imbibition experiments, where the uncovered end of rock samples acted as fracture faces. What's more, a SEM method was used to investigate the pore structures and pore-fill material migration during shut-ins. A NMR method was also been used to investigate the aqueous phase migration during the shut-ins period. By doing this, we wished to uncover the explanation for why well shut-ins and surfactant additives can increase hydrocarbon output.

2.1. Rock Samples

Rock samples of a typical low permeability oil reservoir in the T_1B_1 formation, Mahu Block, Xinjiang Oil Field were selected. These rock samples were drilled out from 3850 m to 3870 m (TVD)

underground. Firstly, porosity was measured with a helium pycometer (KXD-2, Huaxing Petroleum Devices Company, Nantong, China) and permeability was measured with a pulse decay permeability system (STY-2, Huaxing Petroleum Devices Company, Nantong, China) using the nitrogen injection method. In the measurement of permeability, confining pressure and pore pressure were 10 MPa and 7 MPa, respectively. According to the measurements, the average porosity was about 9.0% and the average permeability was about 2.2 mD. Specific physical characters of the rock samples used in our experiments are listed in Table 1.

Table 1. Characters of the original rock samples.

NO.	Diameter/mm	Length/mm	Porosity/%	Permeability/(mD)
1	25.30	29.60	9.75	2.5
2	25.00	29.90	9.33	1.9
3	25.10	29.30	8.29	2.3
4	25.00	29.10	8.81	2.1

Secondly, the mineral composition was detected via the X-ray diffraction (XRD) method using some crushed rock samples Results revealed that quartz, feldspar, calcite, dolomite and clay are the main components, and their proportion are 43.8%, 2.2%, 7.1%, 28.5% and 18.4%, respectively. Lastly, the pore structure was investigated using the constant-rate mercury injection method (ASPE-730, Coretest Systems, Morgan Hill, CA, USA) on a spare core sample from the same formation. From the pore radius distribution map (Figure 1), we can find that the pore radius is mainly concentrated in the interval of 60–300 μm, and is relatively uniform. This may be a reason for the relatively high permeability measured by the nitrogen measurement method.
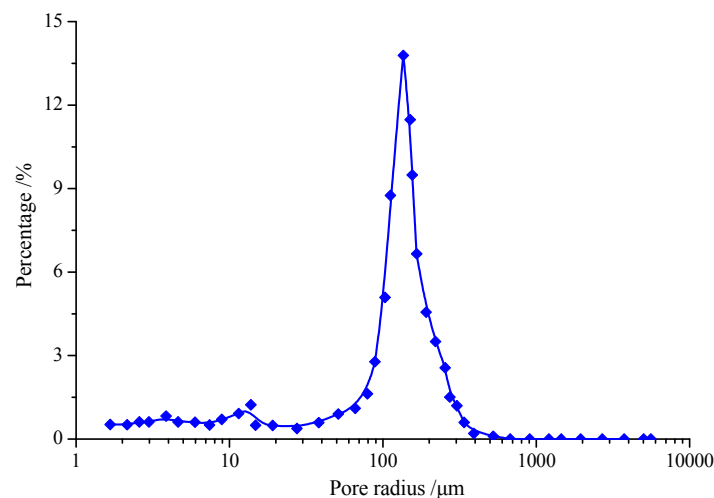

Figure 1. Pore radius distribution map. The pore radius is mainly concentrated in the 60–300 μm interval and relatively uniform.

Thirdly, as shown in Figures 2 and 3, we cut every rock sample into two parts using a waterless cutting method. The waterless cutting machine works slowly and steadily because the diamond wire can easily break, but this method can maintain the original wetting status of rock samples. Then we named the upper part (diameter ≈ 25 mm, thickness ≈ 2 mm) as slices 1# to 4# and the lower part (diameter ≈ 25 mm, height ≈ 26 mm) as core plug 1# to plug 4#. To summarize, we have three different kinds of rock samples in our experiment: rock slices for SEM detection, rock slices for contact angle measurement and rock plugs for imbibition experiments.
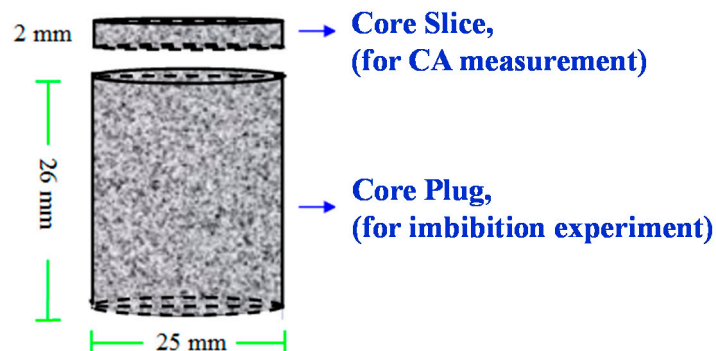
Figure 2. Core sample cutting sketch map. The upper rock slices are used in SEM detection and contact angle measurement, the lower core plugs are used in imbibition test.
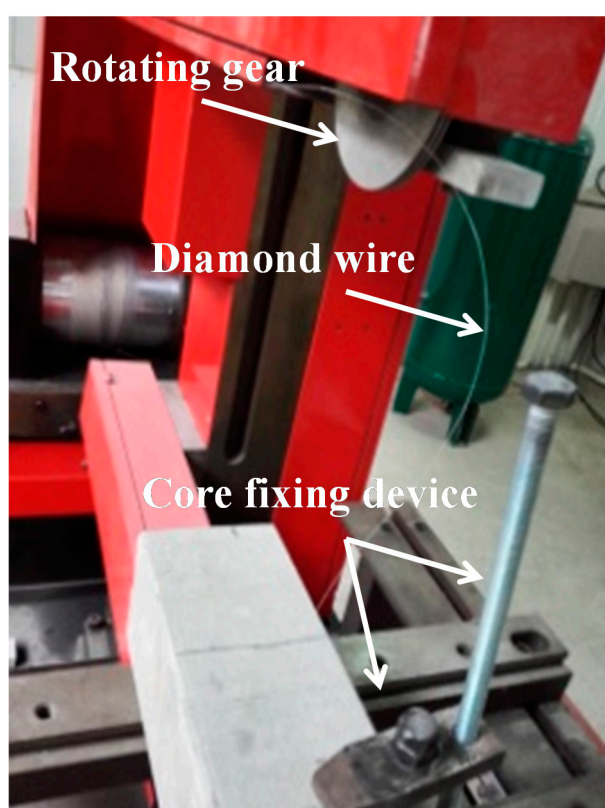

Figure 3. Waterless cutting machine. Waterless cutting methods do not use water as coolant fluid and can keep the rock in the original wetting status.

2.2. Fluids Properties

Here we compound three different kinds of surfactants into slickwater. Octadecyltrimethyl-ammonium chloride TC-8(1831), sodium dodecyl sulfate (K12) and alkyl glucoside APG-0810 were chosen as cationic, anionic and non-ionic surfactants, respectively. Base fluid is slickwater, which is formulated with water, 0.1% mass fraction of hydroxypropyl guar gum (HPG) and 2% mass fraction of KCl.

To differentiate the NMR signals of water from those of oil, a fluorinated oil (Lubricant Oil Company, Beijing, China) was selected as the simulated oil. In the detection, there would no NMR signals from the fluorinated oil, so under these conditions, all signals collected by the NMR apparatus were from the aqueous phase. In this way, aqueous phase migration and original oil distribution in rock samples can be determined by comparing T_2 spectrum differences before and after the shut-ins

period [25]. Another reason for using fluorinated oil is that it doesn't interact with pore rocks and synthetic brine. At 25 °C, the density of fluorinated oil is 1.8 g/cm^3 and the viscosity is 2.1 mPa·s. The mineral ion composition of the synthetic brine is listed in Table 2 and it was used to produce 100% water saturation using a water flooding setup.

Table 2. Mineral ion content of synthetic brine.

Mineral Ions	Na$^+$ + K$^+$	Ca^{2+}	Mg^{2+}	SO$_4{}^{2-}$	Cl$^-$	HCO$_3{}^-$
Ion content/(mg·L^{-1})	2375	16	41	38	1356	1058

2.3. SEM Detection

Rock slices used in SEM detection are cut from the original core plugs using the waterless cutting method. They are square in shape with a side length of 9 mm. We scanned the same position on the rock slice at 600–1600 magnification before and after soaking in slickwater for 100 h. In this way, we can investigate the pore and throat characteristics and intergranular clay mineral characteristics on a microscopic scale. What's more, the influence of shut-ins duration on rock surfaces and mineral particles migration can also be investigated. In this SEM detection process, a QUANTA200 type SEM apparatus (FEI, Eindhoven, The Netherlands) and an INCA350 type energy spectrometer (Oxford Instruments, Oxford, UK) were used and this process is performed at room temperature and pressure.

2.4. NMR Detection Methlodgy

The NMR analyzer is a small and compact apparatus that can be used in the research of pore size distribution, pore water content and pore water migration in geotechnical engineering. In this content, we used a NMR analyzer to investigate aqueous phase migration during shut-ins duration. According to previous studies [26], the relaxation of nuclei in a single channel can be described by the relaxation time and the NMR T_2 spectrum can be expressed using Equation (1):

$$\frac{1}{T_2} = \frac{1}{T_{2B}} + \frac{1}{T_{2S}} + \frac{1}{T_{2D}} \tag{1}$$

where T_2 is total NMR transverse relaxation time; T_{2B} is the bulk relaxation time, which is determined by saturated fluid properties; T_{2S} is the surface relaxation time, which has a high correlation with pore size; T_{2D} is the diffusion relaxation time, which is determined by the molecular diffusion of the fluids.

In our experiments, T_{2D} can be neglected because the magnetic field is homogeneous. T_{2B} can also be neglected when using the same fluids in a specific experiment. Under these circumstances, the T_2 spectrum can be simplified as:

$$\frac{1}{T_2} \approx \frac{1}{T_{2S}} = \rho_2 \left(\frac{S}{V}\right) \tag{2}$$

where, ρ_2 is surface relaxivity, which is a constant for a specific rock sample and is determined by its pore surface properties and mineral composition. S is the interstitial surface area, V is the pore volume. S/V is the surface area, which is in inversely proportional to the pore radius. Therefore, the T_2 spectrum is mainly affected by the pore radius, with a large pore radius corresponding to longer T_2 values while a small pore radius corresponds to shorter T_2 values. Hence, if a relationship between pore radius and T_2 value can be found, the NMR T_2 spectrum can be converted to a pore radius distribution curve and the inside pore structures can be evaluated by the NMR data.

In NMR detection, we measured the T_2 spectrum of one rock sample four different times: after water injection, after oil injection, after 50 h shut-ins and after 90 h shut-ins. During the

NMR measurement, a RecCore-04 type NMR apparatus (Academia Sinica Company, Beijing, China) was used.

2.5. Contact Angle Measurement

Firstly, we polished the surface of core slices 1#~4# with fine sandpaper, and removed small particles and dust using a rubber pipette bulb to ensure the rock surface smooth and clean. Secondly, we put the core slices into simulated oil and aged them for 7 days in an oven at a temperature of 86 °C. This step aimed to make rock samples revert to their oil status. After that, we cleaned their surface using absorbent paper and dried them in an oven at 86 °C for 15 min to eliminate the surface phases. Thirdly, we measured the contact angle using an automated goniometer (DSA100 type, KRUSS Company, Hamburg, Germany, Figure 4.). In this process, a drop (15 µL) of DI water was dripped on the rock sample surface, and the contact angle between the DI water and rock sample was calculated from a camera screenshot. Lastly, we put the rock samples into different kinds of surfactant fluids for 4 days at 86 °C and repeated step 3 to measure the contact angles after surfactant fluid treatment.
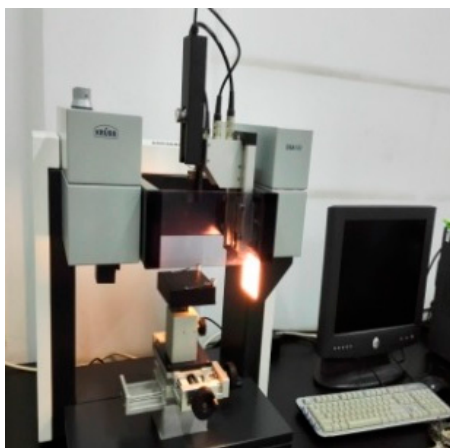

Figure 4. DSA100 type drop shape analyzer.

2.6. IFT Measurement

Here we use a force tension meter (K100 type, KRUSS Company, Hamburg, Germany, Figure 5.) to measure the IFT between simulated oil with base fluids, cationic surfactant, anionic surfactant and non-ionic surfactant at 86 °C.

Figure 5. K100 type force tensiometer.

2.7. OEO Imbibition Experiment

Core plugs 1#~4# are used in the imbibition tests and the following steps are needed to make these rock samples present a lipophilic status initially. Here, a core flooding experiment setup is used and the confining pressure is always 2 MPa larger than the displacement pressure.

Firstly, vacuum is applied and 1PV synthetic brine injected into the rock sample to establish 100% water saturation. Secondly, we inject 10 PV simulated oil into the rock sample at a variable rate, from 0.1 mL/min and 0.2 mL/min to 0.3 mL/min, then age the rock sample for 14 days under the experimental temperature. Thirdly, as shown in Figure 6, we wrap the cylindrical surface and left end surface of the rock sample using resin glue. After that, we put the rock sample into the experimental fluids horizontally to ensure the opened surface is vertically placed. This is a physical model to simulate well shut-ins duration and the open face is used to simulate a fracture face. During this shut-ins period, the aqueous phase imbibed into the rock matrix forms the opened fracture face, and displaces the oil phase out from the opposite direction. This counter-current imbibition is capillary pressure dominated, and there is no gravity influence. During the shut-ins period, we record the weight changes and calculate the imbibition recovery.
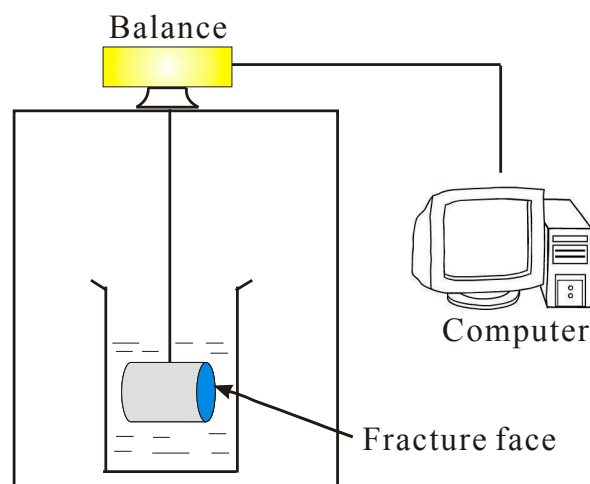

Figure 6. Sketch of the set-up to simulate the shut-ins period. The cylindrical surface and the left end of the rock were sealed, so this is a one end open experiment to simulate well shut-ins and the effect of different surfactant additives.

3. Results

3.1. SEM Results Before and After Soaking

Figure 7 shows core sample SEM images before and after soaking, A1 and A2 are images obtained before soaking while A2 and B2 are images obtained after soaking. From Figure 7 we can find that clay swelling, solid precipitation and fines migration happens after soaking. For example, at Point 1, some less cemented particles migrate to new places, fill and block the original pore spaces. At Point 2, some already existing fractures tend to close up or semi-close up because of clay swelling and rock softening, e.g., the width of one fracture was reduced from 12.93 μm to 11.18 μm for a decrease percentage of 13.5%. These will result in pore space reduction and permeability damage to the rock sample matrix.

At the same time, some new fractures will open as shown at Point 3, while whether these new-open fractures could contribute to effective porosity and permeability is still worth discussing, because they are isolated and not continuous. This can be an intuitive image for porosity and permeability reduction caused by fluid losses and clay swelling during shut-ins, and the high clay content is the reason for this phenomenon.
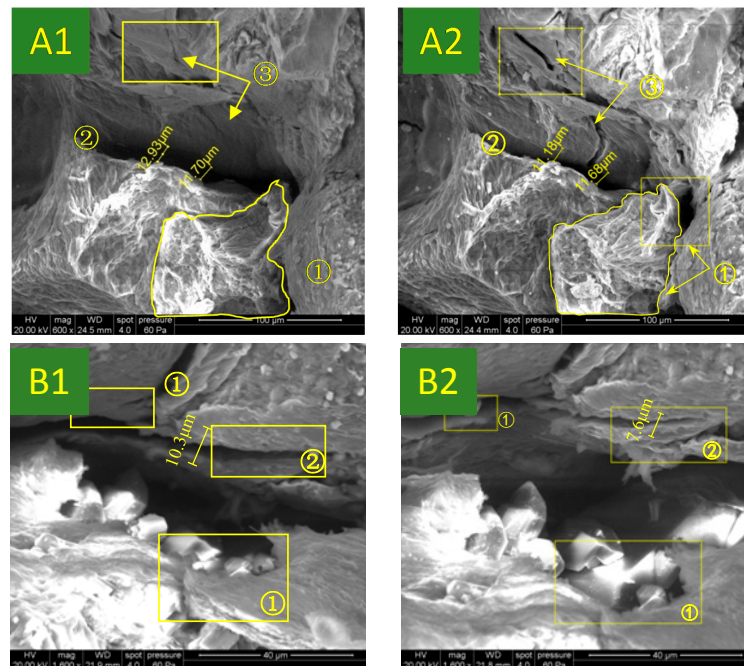
Figure 7. SEM results before and after soaking. (**A1**,**B1**) were detected before soaking, (**A2**,**B2**) were detected after soaking. From the contrast map, we can find that clay swelling, solid precipitation and fines migration happens after the soaking. (**A1**) SEM image of point A before soaking; (**A2**) SEM image of point A after soaking; (**B1**) SEM image of point B before soaking; (**B2**) SEM image of point B after soaking.

3.2. NMR Results before and after Soaking

The T_2 spectrum distribution of the rock sample before and after soaking is shown in Figure 8. The blue line shows 100% water saturatation status and the red line shows the initial oil saturation status. It can be seen that when we inject water into rock samples to establish 100% water saturation, this water distributes in a large interval of 0.2–300 ms with high T_2 amplitude, meaning it occupies both small and large pore spaces, while when we inject simulated oil to reestablish the initial oil saturation, the T_2 amplitude in the 1–100 ms interval decreases from 280 to 145, indicating that water in these intervals is squeezed out by the injected oil.
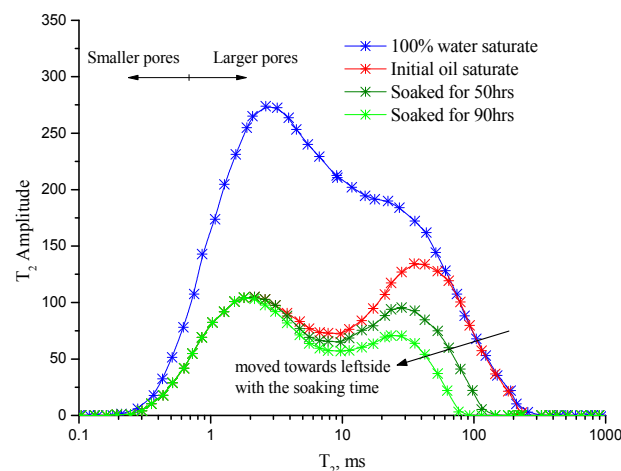

Figure 8. T_2 spectrum shift during the soaking duration. The spectrum shifts towards left during soaking indicating that the aqueous phase migrates from large pore spaces to smaller ones.

In the next step, when turning to the soaking duration, e.g., after 50 h and 90 h' soaking, oil in the interval of 70–300 ms is recovered because the T_2 spectrum shifted from intervals of 300 ms to intervals of 70 ms after 90 h' soaking time. Finally, oil in the intervals of 0.1–10 ms remained in the rock matrix. From the above discussion, the T_2 spectrum shifts towards the left side indicating that the aqueous phase migrates from large pore spaces to smaller ones. We can also say that the main migration direction of the aqueous phase during the soaking is from larger pores to smaller ones. High capillary pressure in smaller pores can be the reason for this phenomenon.

3.3. Contact angle Measure Result

The contact angle of DI water and the initial wetting core slices lies in the interval of 105° and 125°, this phenomenon showing the lipophilic state of the initial rock sample. After surfactant fluid treatment, the contact angle decreased. As shown in Figure 9, the contact angle of core slice 1# (soaked in slickwater) is 103.1°, a decrease of about 20°. The contact angles of core slice 2# (soaked in cationic surfactant), 3# (soaked in nonionic surfactants) and 4# (soaked in anionic surfactant) were 32.6°, 53.9° and 73.4°, decreases of about 75°, 55° and 40°, respectively. The results showed that rock samples present different degrees of wettability alteration after treatment in different kinds of surfactants and cationic surfactants have a much better ability at changing the wettability.
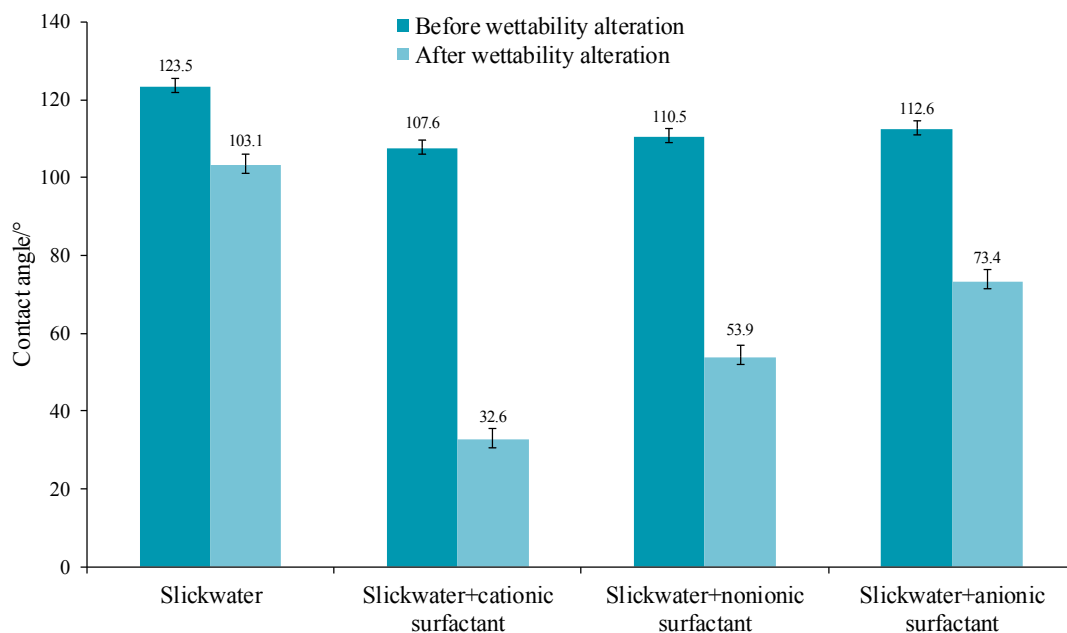

Figure 9. Contact angles before and after wettability alteration. It has shown that cationic surfactants have a better ability in changing rock sample wettability.

3.4. IFT Measurement Result

As shown in Figure 10, IFT between simulated oil and slickwater is 17.26 mN/m, which is the largest. At the same concentration, IFT between simulated oil and anionic surfactant is the lowest, while generally speaking, different kinds of surfactants have a similar ability in lowering IFT and none has a particularly prominent performance. Another phenomenon is the fast IFT decrease with the increase of surfactant concentration for each kind of surfactant.
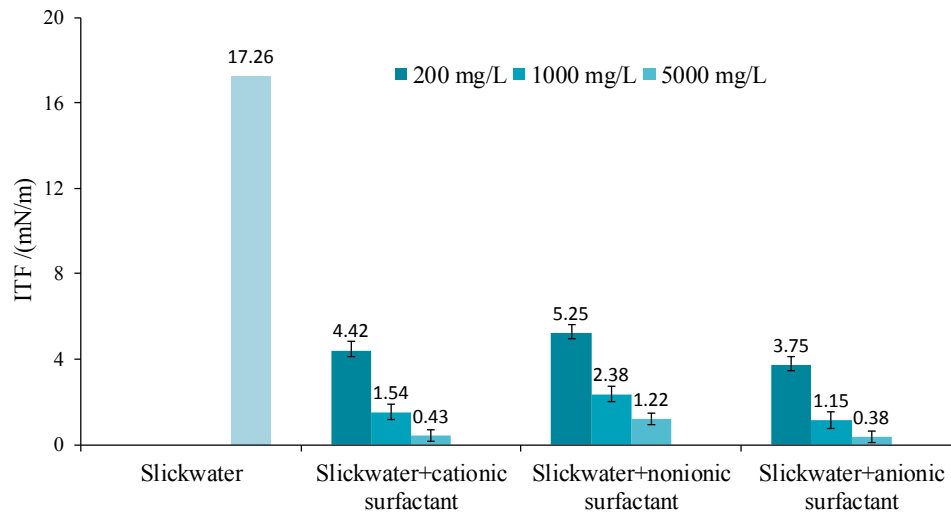
Figure 10. IFT between simulated oil and different fluids. Different kinds of surfactants have a similar ability in lowering IFT, and comparatively, anionic surfactant works a little bit better.

3.5. Imbibition Experiment Results

As shown in Figure 11, for core plug 1#, after soaking in slickwater for 11.4 h, oil began to appear on the uncovered surface. It can also be seen that oil output curve increased slowly and the ultimate oil recovery was only 4.95% after 90 h, while for core plugs 2#~4#, immersed in cationic surfactants, nonionic surfactants and anionic surfactants, respectively, the oil output curves have a similar shape, rising rapidly in the early period and showing a better recovery than core plug 1#.
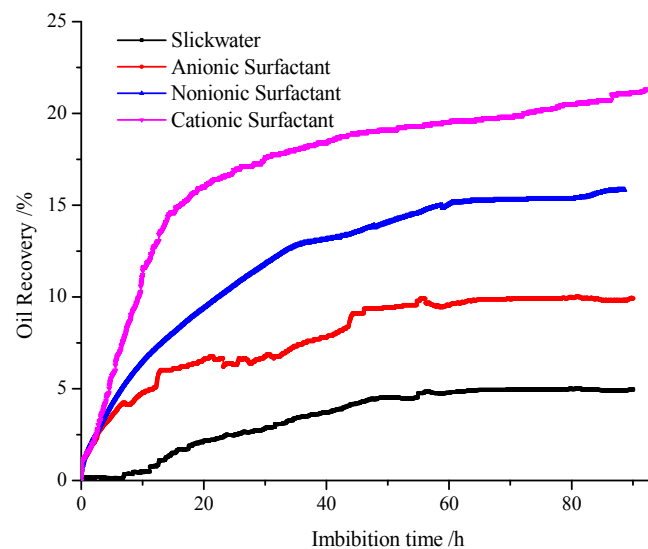

Figure 11. Imbibition recovery of core plugs in different fluids. Cationic surfactant has a better oil recovery than other surfactant additives.

4. Discussion

After the treatment with surfactants, the core samples' wettability changed from hydrophilic to lipophilic which will alter the capillary pressure to an advance force. In addition, IFT decrease may lead the oil phase to move more easily. Here, we use the adhesion reduction factor to evaluate this comprehensive effect. The adhesion reduction factor can be defined as the product of the IFT factor and the wettability factor, and these concepts are defined as follows:

(1) IFT factor:

$$E_\sigma = \frac{\sigma_1}{\sigma_0} \tag{3}$$

where, E_σ is IFT factor, dimensionless; σ_1 is IFT between surfactants and simulated oil, mN/m, σ_0 is IFT between slickwater and simulated oil, mN/m;

(2) Wettability factor:

$$E_\theta = \frac{1 - \cos\theta_1}{1 - \cos\theta_0} \tag{4}$$

where, E_θ is wettability factor, dimensionless; θ_1 is contact angle of DI water on rock surface after soaking period, degree; θ_0 is contact angle of DI water on rock surface before soaking period, degree.

(3) Adhesion reduction factor

In the imbibition process, the oil phase has to conquer the adhesion resistance to move from one place to another and this adhesion work is related to the IFT and contact angle. As described above, we define the adhesion reduction factor using Equation (5):

$$E_A = E_\sigma E_\theta = \frac{\sigma_1}{\sigma_0} \frac{1 - \cos\theta_1}{1 - \cos\theta_0} \tag{5}$$

Finally, we put all experimental data into Table 3 and draw it in Figure 12. As shown in Figure 13, we put the imbibition recovery, IFT factor, wettability factor and adhesion reduction factor into a logarithmic coordinate system. We can see that, even though the anionic surfactant can decrease IFT to a better level, the ultimate imbibition recovery is still dependent on the adhesion reduction factor. Cationic surfactant additives have the lowest adhesion reduction factor while also the largest oil recovery. The ultimate imbibition recovery and adhesion reduction factor maintains an inverse proportion, the lower the adhesion reduction factor, the higher the imbibition recovery.

Table 3. Experiment results of surfactant additivities in the OEO imbibition process.

NO.	Fluids	Surface Tension/(mN·m^{-1})	IFT/(mN·m^{-1})	θ_0/°	θ_1/°	E_σ	E_θ	E_A	IOR/%
1#	Slickwater	60.61	17.26	123.5	103.1	1.000	0.79	0.790	4.95
2#	Slickwater + cationic surfactant	32.20	0.43	107.6	32.6	0.025	0.12	0.003	21.29
3#	Slickwater + non-ionic surfactant	29.21	1.22	110.5	53.9	0.071	0.30	0.021	9.91
4#	Slickwater + anionic surfactant	29.78	0.38	112.6	73.4	0.022	0.51	0.011	15.84

Previous studies have revealed that during hydraulic fracturing, fluid losses and water invasion may cause permeability and hydrocarbon production damage [27]. Figure 13 is a schematic map of fluid loss and water invasion during hydraulic fracturing. Studies have revealed that this invading water is mainly distributed near horizontal wells and hydraulic fracture faces [5–8]. These aqueous phases occupy large amounts of the pore spaces that originally belonged to the oil phase. The consequences of this situation are pore space discontinuity, capillary discontinuity and 2-phase seepage resistance. Afterwards this will lead to a huge pressure drop in the depletion development process. Our experiment has demonstrated that both well shut-ins and surfactant additivities can improve oil output during hydraulic fracturing. As illustrated in the NMR results, during the well shut-ins period, aqueous phases redistribute and migrate to smaller pore spaces and deeper distances via capillary dominated counter-current imbibition. In this way, near-fracture water-blocks can be removed by well shut-ins and a smooth and fluent channel for oil phase flow can be formed accompanying the reduction of aqueous phase in pore spaces. What's more, when the aqueous phase is imbibed into formation pore spaces, water saturation decreases which will result in an increase of oil relative permeability. Near fracture water-block removal may be the most direct reason for high hydrocarbon output after hydraulic fracturing shut-ins.
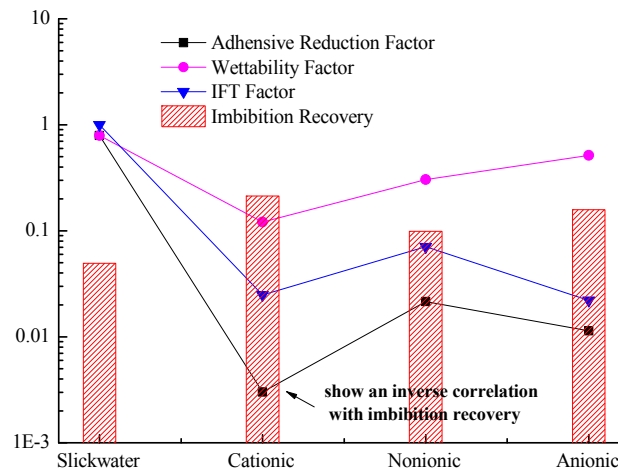
Figure 12. Performance of different liquids. Ultimate imbibition recovery and adhesion reduction factor maintain an inverse proportion, the lower the adhesion reduction factor, the higher the imbibition recovery.
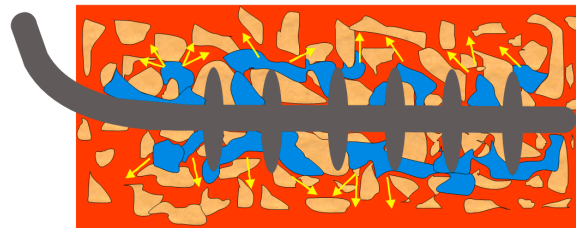

Figure 13. Scheme map of water-block removal. Near fracture water-block removal may be the most direct reason for high hydrocarbon output after hydraulic fracturing shut-ins.

It is worth mentioning that well shut-ins can last for several months or more during actual industry operation and such a long time may cause serious economic problems. Our experiment has also showed that surfactant additives can accelerate the water-block removal procedure through the promotion of aqueous migration. This is mainly due to wettability alteration and an IFT reduction mechanism. When core samples changed to water-wet after soaking in surfactants, the capillary force turned to an advance force for spontaneous imbibition. In addition, IFT reduction caused by surfactants can reduce capillary trap forces, which will make oil and aqueous phases move easier in pores and throats. In this way, surfactant additives accelerate the velocity of aqueous redistribution and water-block removal. It should also be noted that in industry operation, large amounts of cationic surfactant will be adsorbed onto the negative charged pore surfaces, so high concentrations are needed and the economic issues of using cationic surfactant additivities should also be considered.

5. Conclusions

(1) Cationic surfactants have better IOR performance in OEO imbibition experiment due to their high wettability alteration ability on vertical fracture faces. The adhesion factor is an effective evaluation parameter, and the lower the adhesion factor, the higher the imbibition recovery.

(2) During the soaking duration, the aqueous phases redistribute and migrate to smaller pore spaces and deeper distances via an imbibition mechanism. Thus, water-blocks distributed near the fracture face can be removed and this process can be enhanced by surfactant additives. Near fracture water-block removal may be the most direct reason for the high hydrocarbon outputs observed after well shut-ins.

(3)   NMR results also showed that the recovered oil was mainly distributed in intervals of 10–300 ms while the oil remaining unrecovered was mainly distributed in intervals of 0.1–10 ms. New technology that can recover hydrocarbons in these smaller pores should be promoted.

Author Contributions: Yunhong Ding and Shuai Li designed the research; Shimin Liu and Jun Tang performed the research; Bo Cai and Guangfeng Liu analyzed core flooding experimental data; Shuai Li and Guangfeng Liu analyzed NMR detection data.

Conflicts of Interest: The authors declare that they have no competing interests.

Nomenclature

T_2	total relaxation time, ms
T_{2B}	bulk relaxation time, ms
T_{2S}	surface relaxation time, ms
T_{2D}	diffusion relaxation time, ms
ρ_2	surface relaxivity, $\mu m/ms$
S	interstitial surface area, μm^2
V	pore volume, μm^3
E_σ	IFT factor, dimensionless
σ_1	IFT between surfactants and simulated oil, mN/m
σ_0	IFT between slickwater and simulated oil, mN/m
E_θ	wettability factor, dimensionless
θ_1	contact angle of water on rock surface after wettability alteration, degree
θ_0	contact angle of water on rock surface before wettability alteration, degree
E_A	adhesion reduction factor, dimensionless

References

1.   Jacot, R.H.; Bazan, L.W.; Meyer, B.R. Technology Integration: A Methodology to Enhance Production and Maximize Economics in Horizontal Marcellus Shale Wells. In Proceedings of the SPE Annual Technical Conference and Exhibition, Florence, Italy, 19–22 September 2010.

2.   Qi, W.; Yun, X.; Xiaoquan, W.; Tengfei, W.; Zhang, S. Volume fracturing technology of unconventional reservoirs: Connotation, design optimization and implementation. *Pet. Explor. Dev.* **2012**, *39*, 377–384. [CrossRef]

3.   Shuai, L.; Yunhong, D.; Bo, C.; Yongjun, L. Experiment and Modelling of Massive Fracturing Considering Drainage and Imbition Process in Tight Oil Reservoirs. In Proceedings of the International Petroleum Technology Conference, Bangkok, Thailand, 14–16 November 2016.

4.   Sheng, J. *Modern Chemical Enhanced Oil Recovery: Theory and Practice*; Gulf Professional Publishing: Houston, TX, USA, 2010; pp. 247–277, ISBN 978-1-85617-745-0.

5.   Zhang, D.L.; Liu, S.; Puerto, M.; Miller, C.A.; Hirasaki, G.J. Wettability alteration and spontaneous imbibition in oil-wet carbonate formations. *J. Pet. Sci. Eng.* **2006**, *52*, 213–226. [CrossRef]

6.   Zhou, Z.; Abass, H.; Li, X.; Teklu, T. Experimental investigation of the effect of imbibition on shale permeability during hydraulic fracturing. *J. Nat. Gas Sci. Eng.* **2016**, *29*, 413–430. [CrossRef]

7.   Harrison, A.L.; Jew, A.D.; Dustin, M.K.; Thomas, D.L.; Joe-Wong, C.M.; Bargar, J.R.; Johnson, N.; Brown, G.E.; Maher, K. Element release and reaction-induced porosity alteration during shale-hydraulic fracturing fluid interactions. *Appl. Geochem.* **2017**, *82*, 47–62. [CrossRef]

8.   Liang, T.; Longoria, R.A.; Lu, J.; Nguyen, Q.P.; DiCarlo, D.A. Enhancing hydrocarbon permeability after hydraulic fracturing: Laboratory evaluations of shut-ins and surfactant additives. *SPE J.* **2017**, *22*, 1011–1023. [CrossRef]

9.   Ahmadi, M.; Sharma, M.M.; Pope, G.; Torres, D.E.; McCulley, C.A.; Linnemeyer, H. Chemical treatment to mitigate condensate and water blocking in gas wells in carbonate reservoirs. *SPE Prod. Oper.* **2011**, *26*, 67–74. [CrossRef]

10. Almulhim, A.; Alharthy, N.; Tutuncu, A.N.; Kazemi, H. Impact of imbibition mechanism on flowback behavior: A numerical study. In Proceedings of the Abu Dhabi International Petroleum Exhibition and Conference, Abu Dhabi, UAE, 10–13 November 2014.

11. Das, P.; Achalpurkar, M.; Pal, O. Impact of Formation Softening and Rock Mechanical Properties on Selection of Shale Stimulation Fluid: Laboratory Evaluation. In Proceedings of the SPE/EAGE European Unconventional Resources Conference and Exhibition, Vienna, Austria, 25–27 February 2014.

12. Cheng, Y. Impact of water dynamics in fractures on the performance of hydraulically fractured wells in gas-shale reservoirs. *J. Can. Pet. Technol.* **2012**, *51*, 143–151. [CrossRef]

13. Dutta, R.; Lee, C.H.; Odumabo, S.; Ye, P.; Walker, S.C.; Karpyn, Z.T.; Ayala, H.; Luis, F. Experimental investigation of fracturing-fluid migration caused by spontaneous imbibition in fractured low-permeability sands. *SPE Reserv. Eval. Eng.* **2014**, *17*, 74–81. [CrossRef]

14. Bertoncello, A.; Wallace, J.; Blyton, C.; Honarpour, M.; Kabir, C.S. Imbibition and Water Blockage in Unconventional Reservoirs: Well-Management Implications during Flowback and Early Production. *SPE Reserv. Eval. Eng.* **2014**, *17*, 497–506. [CrossRef]

15. Alvarez, J.O.; Schechter, D.S. Wettability alteration and spontaneous imbibition in unconventional liquid reservoirs by surfactant additives. In Proceedings of the SPE Latin American and Caribbean Petroleum Engineering Conference, Quito, Ecuador, 18–20 November 2016.

16. Shuai, L.; Bo, C.; Yunhong, D.; Yongjun, L.; Chunming, H. Damage of Fracture Face Skin in Massive Hydraulic Fracture Stimulation. In Proceedings of the IADC/SPE Asia Pacific Drilling Technology Conference, Singapore, 22–24 August 2016.

17. Wang, X.; Xiao, S.; Zhang, Z.; He, J. Effect of Nanoparticles on Spontaneous Imbibition of Water into Ultraconfined Reservoir Capillary by Molecular Dynamics Simulation. *Energies* **2017**, *10*, 506. [CrossRef]

18. Standnes, D.C.; Austad, T. Wettability alteration in chalk: 2. Mechanism for wettability alteration from oil-wet to water-wet using surfactants. *J. Pet. Sci. Eng.* **2000**, *28*, 123–143. [CrossRef]

19. Hirasaki, G.; Zhang, D.L. Surface chemistry of oil recovery from fractured, oil-wet, carbonate formations. *SPE J.* **2004**, *9*, 15–62. [CrossRef]

20. Hou, B.; Wang, Y.; Cao, X.; Zhang, J.; Song, X.; Ding, M.; Chen, W. Mechanisms of enhanced oil recovery by surfactant-induced wettability alteration. *J. Dispers. Sci. Technol.* **2016**, *37*, 1259–1267. [CrossRef]

21. Chen, H.L.; Lucas, L.R.; Nogaret, L.A.D.; Yang, H.D.; Kenyon, D.E. Laboratory monitoring of surfactant imbibition using computerized tomography. In Proceedings of the SPE International Petroleum Conference and Exhibition in Mexico, Villahermosa, Mexico, 1–3 February 2000.

22. Bazin, B.; Peysson, Y.; Lamy, F.; Martin, F.; Aubry, E.; Chapuis, C. In-situ water-blocking measurements and interpretation related to fracturing operations in tight gas reservoirs. *SPE Prod. Oper.* **2010**, *25*, 431–437. [CrossRef]

23. Li, S.; Ding, Y.H.; Cai, B.; Lu, Y.; Gu, D. Solution for counter-current imbibition of 1D immiscible two-phase flow in tight oil reservoir. *J. Pet. Explor. Prod. Technol.* **2016**, *7*, 727–733. [CrossRef]

24. Sun, Y.; Bai, B.; Wei, M. Microfracture and surfactant impact on linear cocurrent brine imbibition in gas-saturated shale. *Energy Fuels* **2015**, *29*, 1438–1446. [CrossRef]

25. Yang, P.; Guo, H.; Yang, D. Determination of residual oil distribution during waterflooding in tight oil formations with NMR relaxometry measurements. *Energy Fuels* **2013**, *27*, 5750–5756. [CrossRef]

26. Liu, D.; Ge, H.; Liu, J.; Shen, Y.; Wang, Y.; Liu, Q.; Jin, C.; Zhang, Y. Experimental investigation on aqueous phase migration in unconventional gas reservoir rock samples by nuclear magnetic resonance. *J. Nat. Gas Sci. Eng.* **2016**, *36*, 837–851. [CrossRef]

27. Alramahi, B.; Sundberg, M.I. Proppant embedment and conductivity of hydraulic fractures in shales. In Proceedings of the 46th US Rock Mechanics/Geomechanics Symposium, Chicago, IL, USA, 24–27 June 2012.